Tribology Letters, Vol. 18, No. 2, February 2005 (© 2005)
DOI: 10.1007/s11249-004-1769-4

Effectiveness of an externally added solid lubricant on the sliding wear response of a zinc–aluminium alloy, its composite and cast iron

B.K. Prasad*

Regional Research Laboratory (CSIR), Bhopal 462 026, India

Received 13 June 2004; accepted 2 August 2004

The role played by an externally added solid lubricant like graphite towards controlling the sliding wear behaviour of a zinc-based alloy has been examined in this study. The influence of dispersing hard silicon carbide particles in the alloy was also investigated by testing the composite in identical test conditions. The wear performance of the zinc-based alloy and its composite was compared with that of a gray cast iron. Wear tests were performed in oil lubricated environment. Composition of the lubricant was changed by adding various quantities of graphite (particles) to the oil. The study suggests that the wear response (in terms of wear rate, frictional heating and friction coefficient) of the samples improved in the presence of suspended graphite particles in the oil lubricant. However, this improvement was noticed up to a critical content of graphite particles only and the trend reversed at still higher graphite contents. The zinc-based (matrix) alloy revealed highest wear rate. Dispersoid silicon carbide particles showed a significant improvement in the wear performance of the matrix alloy. The cast iron performed in between the matrix alloy and composite. The frictional heating and friction coefficient were the highest for the composite while the cast iron and the matrix alloy showed a mixed response. Examinations of wear surfaces, subsurface regions and debris particles helped to substantiate the observed wear response of the samples.

KEYWORDS: cast iron, zinc-based alloy and composite, lubricated sliding wear behaviour, solid lubricant, microstructure-wear property correlations

1. Introduction

Zinc-based alloys have been found to have potential to substitute for a variety of ferrous and non-ferrous alloys in several engineering applications involving sliding action in the presence of a liquid (oil) lubricant [1–3]. Dispersion of hard ceramic particles like silicon carbide has been observed to improve the mechanical and sliding wear properties of the zinc-based alloys [4–12]. Gray cast iron components are widely used in sliding wear applications [13–16]. Presence of solid lubricants like graphite has been observed to improve the wear performance of materials such as cast irons [13,17–19] while a mixed response has been observed in the case of aluminium alloys [20–28]. The wear performance is affected by the nature, type and the content of the solid lubricant [17–19,23–44]. The solid lubricants can serve the purpose either by being present within the material system [17–19,23–44] or by being added externally in between the contacting surfaces independently [45,46] or along with a semi-solid/liquid lubricant. It has been observed that the benefits of adding a solid lubricant as a microconstituent in the material system itself [17–19,23–44] very much depends on factors concerning the test material and conditions that favour effective smearing of the lubricant phase on the contacting surfaces and those which lead to premature removal of the phase through flaking and cracking from the sliding surfaces [17–44]. The predominance of one set of factors over the other actually dictates the role of the (lubricating) phase towards controlling the overall wear response of materials in specific test conditions [17–36,47]. Moreover, a solid lubricant phase when present within the material system adversely affects mechanical strength and that is undesirable [23,45]. Accordingly, a more effective way of making use of the solid lubricants in sliding applications (without any adverse effects on material properties) may be to add them directly in between the contacting surfaces either independently [45,46] or along with a semi-solid/liquid lubricant. As far as the influence of the solid lubricant phase (when added externally along with a semi-solid/liquid lubricant) on wear behaviour is concerned, the content of the phase in the lubricant mixture, viscosity of the lubricant mixture, tendency of the phase to form agglomerates in the mixture and adhering characteristics of the phase onto the sliding surfaces [30,31,43,44] are expected to govern the wear behaviour of materials. This opens a wide area of research to be carried out towards developing a systematic understanding of the influence of these factors on wear behaviour. However, practically no information seems to be available as far as the effect of suspended solid lubricant particles in oil lubricants

*E-mail: braj_kprasad@yahoo.co.in

on the sliding wear characteristics of zinc-based alloys, composites and cast irons is concerned. Moreover, the influence of the content of solid lubricant particles in the oil lubricant on the wear response of the materials also does not seem to have been studied.

In view of the above, an attempt has been made in this investigation to examine the effects of adding varying quantities of a widely used solid lubricant like graphite particles to an oil lubricant on the wear performance of a zinc-based alloy. The influence of the dispersoid silicon carbide particles on the wear behaviour of the zinc-based alloy was studied by testing the composite in identical conditions. The wear properties of the matrix alloy and composite were compared with those of a gray cast iron. Wear surfaces, subsurface regions and debris particles were also examined for further substantiating the wear behaviour of the samples.

2. Experimental

2.1. Material preparation

The experimental alloys and composite were prepared by the liquid metallurgy route in the form of 20 mm diameter, 150 mm long cylindrical castings. The composite was synthesized by dispersing 50–100 μm silicon carbide particles at the vortex of the alloy melt. Table 1 shows the chemical compositions of the sample materials.

2.2. Microstructural examination

Microstructural studies were carried out on 20 mm diameter, 15 mm thick samples. The samples were polished metallographically and etched suitably. Diluted aqua regia was used for etching the samples of the zinc-based (matrix) alloy and composite while the cast iron was etched with 2% nital solution. Microstructural characterization of the samples was carried out using optical and scanning electron microscopy.

2.3. Measurement of hardness and density

Hardness measurements were carried out on metallographically polished samples using a Vickers hardness tester. The applied load in this case was 30 kg. The water displacement technique was adopted for density measurement. A Mettler microbalance was used for weighing the samples in water and air.

2.4. Sliding wear tests

Lubricated sliding wear tests were carried out using a DUCOM pin-on-disc machine. Varying quantities of 50–100 μm graphite particles in the range of 0–10% were suspended in SAE 40 oil by thoroughly mixing the two mechanically. The disc was made of an En31 steel (1.02% C, 1.05% Cr, 0.3% Ni, 0.35% Mn and balance Fe) having hardness Rc 62. A schematic representation of the wear test configuration is shown in figure 1. The pin samples used for the tests were 8 mm in diameter and 30 mm in length. Prior to testing, the pin samples and the disc were polished metallographically to a roughness (Ra) level of 0.8 μm (where Ra is the arithmetic mean of departure of the surface roughness profile from the mean line). Roughness measurements were carried out using a Rank Taylor Hobson (RTH 6) profilometer. The polished disc was immersed in the lubricant and allowed to rotate at a speed of 2.68 m/s for 5 s prior to initiating the tests. The pin sample was then pressed against the disc by applying load with the help of dead weights through a cantilever mechanism. The applied load, sliding distance and sliding speed in this study were fixed at 14 kg, 2500 m and 2.68 m/s,

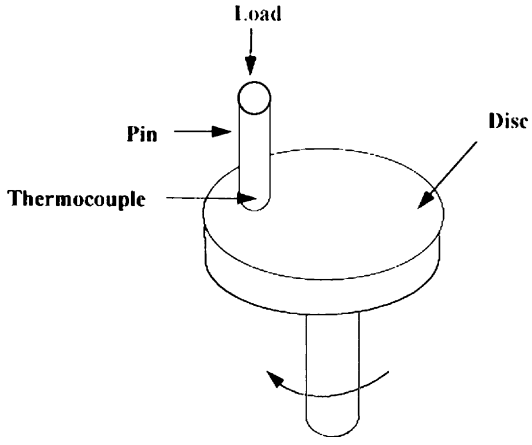

Figure 1. A schematic representation of the wear test configuration.

Table 1.
Chemical compositions of the sample materials.

Sample	Weight %, Element									
	Fe	Zn	Al	Si	Cu	Mg	Mn	C	P	S
Cast iron	*	–	–	2.58	–	–	0.49	3.25	0.09	0.07
Zinc-based (matrix) alloy	–	*	37.5	–	2.5	0.2	–	–	–	–
Composite	Matrix alloy dispersed with 10 wt% SiC particles									

*remainder

respectively. Temperature near the specimen surface was monitored during the wear tests by inserting a chromel–alumel thermocouple in a hole made at a distance of 1.5 mm from the contacting surface of the pin. The samples were weighed prior to and after testing using a Mettler microbalance. Friction coefficient during the tests was measured with the help of a force transducer. The samples were cleaned well with carbon tetrachloride and acetone prior to and after the wear tests.

2.5. *Examination of wear surfaces, subsurface regions and debris*

Wear surfaces, subsurface regions and debris particles were studied using a JEOL 5600 scanning electron microscope (SEM). The samples were mounted on brass studs and sputtered with gold prior to their SEM studies. Sections normal to the wear surfaces in the sliding direction were mounted in polyester resin, polished metallographically and etched suitably prior to mounting on the brass studs. The zinc-based alloy and composite were etched with diluted aqua regia while 2% nital solution was used for etching the cast iron samples. The debris particles were suspended in carbon tetrachloride and then in acetone to remove the oily substance from them. They were then spreaded on a glass slide and fixed on a brass stud with the help of a double-sided adhesive tape.

3. Results and discussion

3.1. *Microstructure*

Figure 2 shows microstructural features of the samples. The zinc-based (matrix) alloy revealed primary α

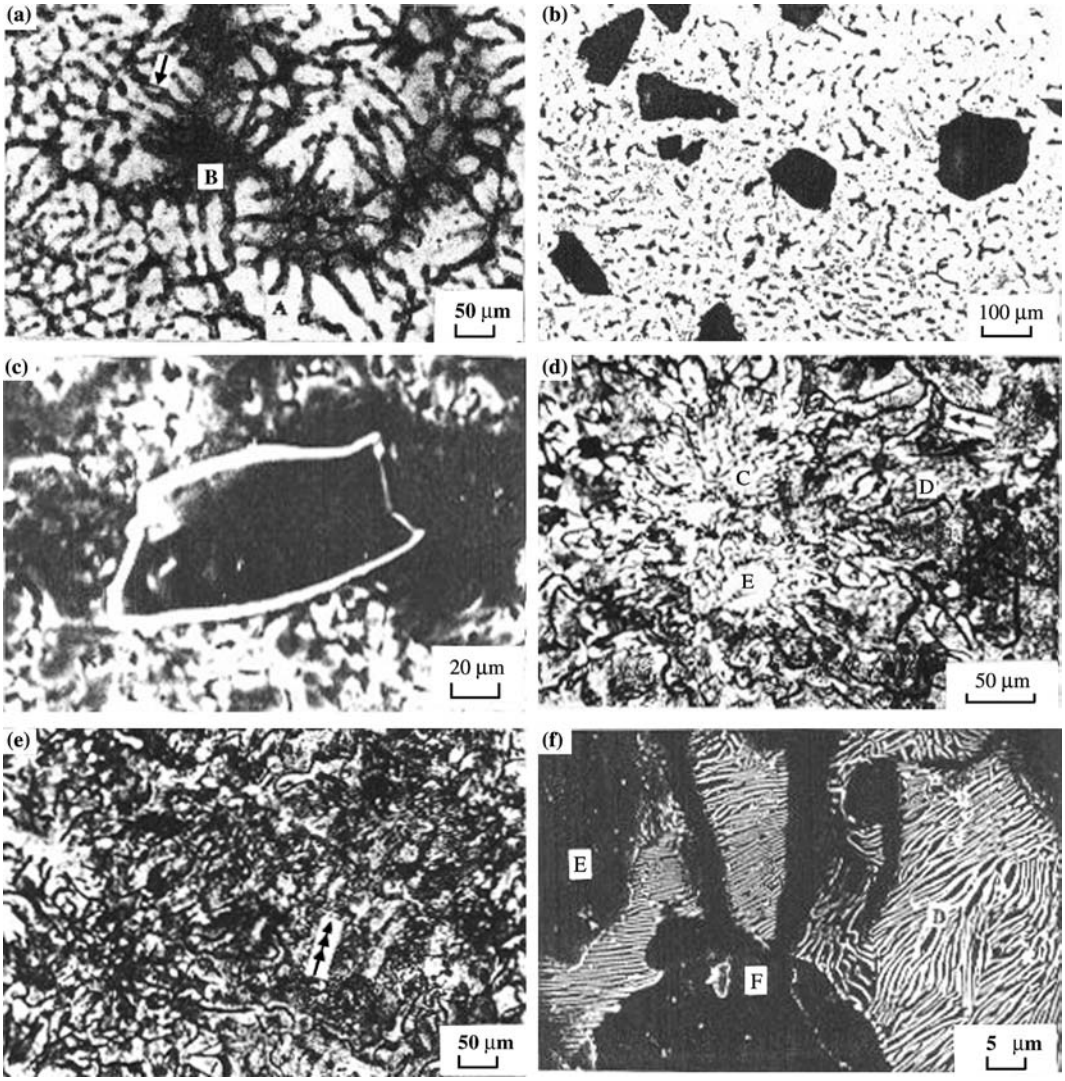

Figure 2. Microstructure of (a) zinc-based (matrix) alloy, (b and c) composite and (d–f) cast iron [A: primary α, B: eutectoid $\alpha + \eta$, single arrow: ε, double arrow: graphite flake, triple arrow: interdendritic segregation of graphite, C: rosettes of graphite, D: pearlite, E: ferrite,F: decohesion of graphite at graphite/ferrite interface].

dendrites, surrounded by the eutectoid $\alpha + \eta$ and metastable ε phase (figure 2(a), regions marked by A, B and a single arrow respectively). The composite showed reasonably uniform distribution of the dispersoid silicon carbide particles in the matrix (figure 2(b)). Dispersoid/matrix interfacial bonding was noted to be fairly sound (figure 2(c)). The matrix part of the composite (figure 2(b)) showed features practically identical to those of the zinc-based (matrix) alloy (figure 2(a)). The cast iron revealed different modes of distribution of graphite such as a random distribution of coarse distorted flakes and rosettes of fine flakes (figure 2(d), regions marked by a double arrow and C respectively). Interdendritic segregation of fine flakes of graphite was also noticed (figure 2(e), region marked by a triple arrow). The size of the graphite phase also varied widely (region marked by a double arrow versus C in figure 2(d)). The matrix part of the cast iron comprised pearlite along with a limited quantity of ferrite (figure 2(d), regions marked by D and E respectively). A magnified view clearly reveals the ferrite and pearlite phases (figure 2(f), regions marked by D and E, respectively). Occasional decohesion of graphite phase was observed at the ferrite/graphite interface (figure 2(f), region marked by F). Aspects concerning the mode of formation of various microconstituents, their characteristic features controlling the wear response of the samples and the solidification behaviour of the alloys have been discussed elsewhere [4,8,13,14,17–47,46–71].

3.2. Hardness and density

Table 2 shows the hardness and density of the samples. The cast iron attained highest density followed by that of the (zinc-based) matrix alloy and composite. Hardness of the matrix alloy was the least while that of the cast iron the maximum, the composite attaining a hardness value intermediate between the two.

3.3. Wear behaviour

Wear rate of the samples has been plotted as a function of graphite particle content suspended in the oil lubricant (figure 3). Increasing content of graphite particles led to a reduction of the wear rate initially. This was followed by the attainment of the wear rate

Table 2.
Density and hardness of the samples.

Sample	Density, g/cc	Hardness, HV
Cast iron	6.99	220
Zinc-based (matrix) alloy	4.41	135
Composite	4.37	162

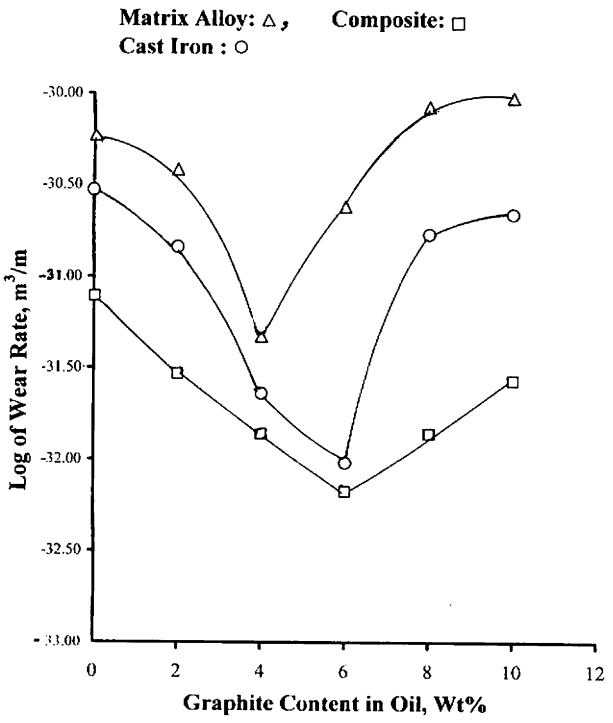

Figure 3. Wear rate of the samples plotted as a function of graphite content in the oil lubricant.

minimum and then a reversal in the trend at still higher contents of graphite in the lubricant mixture. The zinc-based (matrix) alloy suffered from maximum wear rate while that of the composite was the least, the response of the cast iron being intermediate between the two. The critical content of suspended graphite particles leading to minimum wear rate was noted to be 4% for the matrix alloy and 6% for the cast iron and composite samples.

Temperature near the specimen surface has been plotted in figure 4 as a function of test duration. The influence of suspended graphite particles in the oil lubricant is also evident from the figure. Frictional heating increased with test duration. The rate of frictional heating was high in the beginning of the tests. This was followed by a reduced rate of temperature increase at still longer test durations. Frictional heating got reduced as a result of graphite addition to the oil lubricant. The matrix alloy showed a dramatic reduction in its frictional heating in this case. Moreover, in the oil-only lubricated tests, the matrix alloy experienced maximum frictional heating while the cast iron revealed the least, the composite attaining an intermediate response. In the oil-plus-graphite environment, the highest frictional heating was observed for the composite followed by that of the cast iron and the matrix alloy.

Maximum temperature near the specimen surface is shown in figure 5 as a function of graphite content of the oil lubricant. The frictional heating got reduced

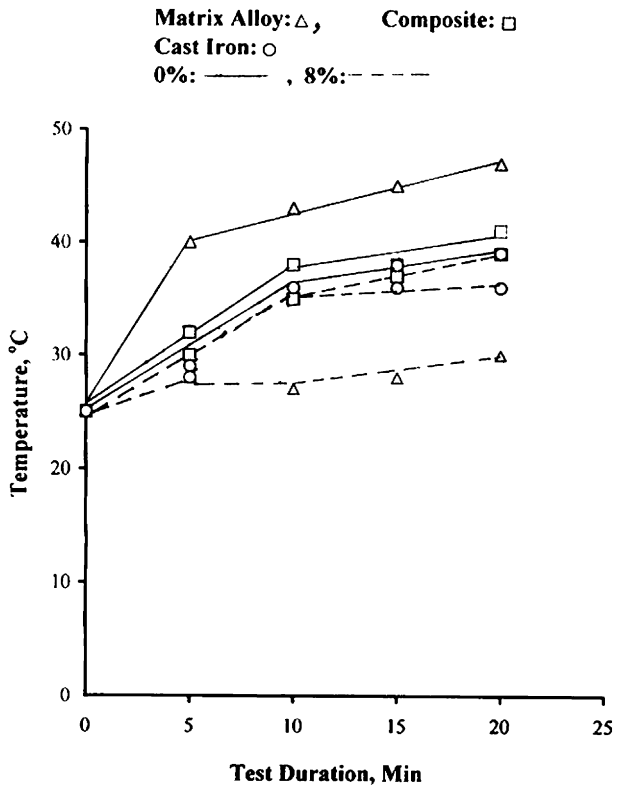

Figure 4. Temperature near the contacting surface of the samples as a function of test duration (solid lines: oil plus 0% graphite particles, dashed lines: oil plus 8% graphite particles).

with increasing content of graphite, attained the minimum at specific graphite content and then showed a reversal in the trend at still higher concentrations of graphite in the oil lubricant. The composite demonstrated maximum frictional heating while the cast iron attained frictional heating comparable to that of the matrix alloy.

Friction coefficient of the samples has been plotted as a function of test duration in figure 6. The test duration marginally affected the friction coefficient of the zinc-based (matrix) alloy except in the case of oil plus graphite mixture towards the end of the test. The friction coefficient increased with test duration in the case of the cast iron, attained a maximum and then decreased once again at longer test durations. The composite also followed a trend similar to that of the cast iron when tested in oil plus graphite environment while the trend reversed in the oil lubricant alone at least initially. The matrix alloy showed the minimum friction coefficient followed by that of the cast iron and composite. The suspended graphite particles in the oil lubricant caused the friction coefficient to decrease.

Steady state friction coefficient has been plotted in figure 7 as a function of graphite particle concentration in the oil lubricant. The friction coefficient got reduced with increasing graphite content and attained a minimum at a specific content of graphite. The trend reversed at still higher concentrations of graphite particles. The composite attained the highest friction coefficient irrespective of the graphite content. A mixed response was observed by the cast iron and zinc-based (matrix) alloy. For example, the friction coefficient of

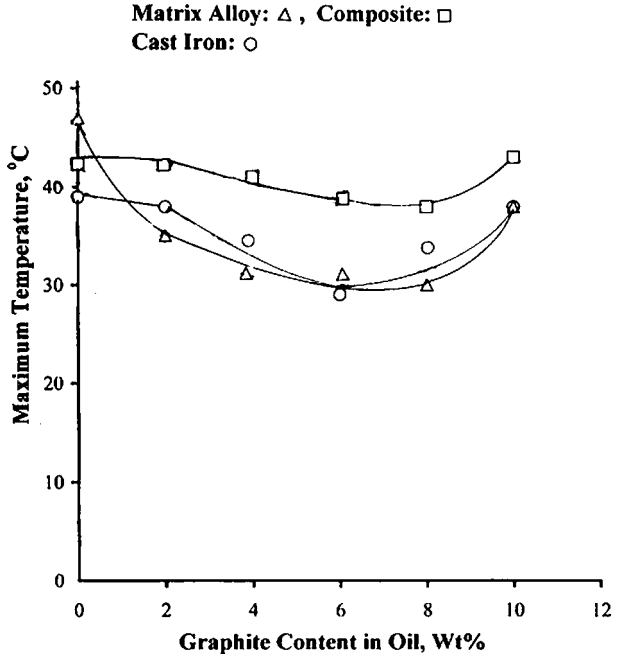

Figure 5. Maximum temperature near the sliding surface of the samples as a function of graphite content in the oil lubricant.

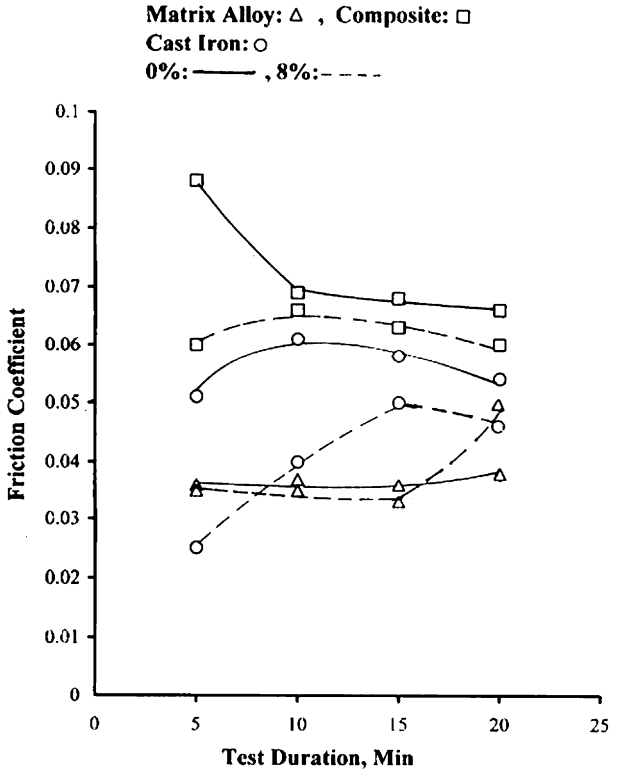

Figure 6. Friction coefficient of the samples plotted as a function of test duration (solid lines: oil plus 0% graphite particles, dashed lines: oil plus 8% graphite particles).

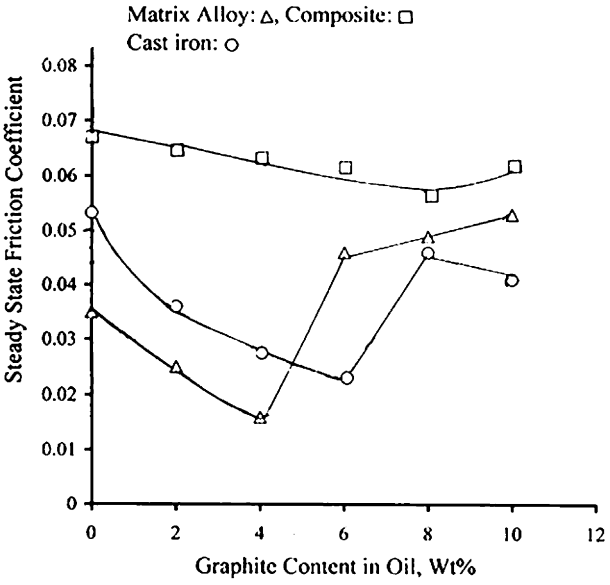

Figure 7. Steady state friction coefficient of the samples versus graphite content in the oil lubricant.

the zinc-based (matrix) alloy was less than that of the cast iron up to a critical content of graphite in the oil while a reverse trend was noticed at still higher graphite concentrations.

3.4. Wear surfaces

Wear surfaces of the samples are shown in figure 8. The zinc-based (matrix) alloy showed its wear surface to contain fine grooves when tested in oil alone (figure 8(a)). The presence of graphite in the oil lubricant caused the wear surface to be relatively smoother (figure 8(b)) than that in the case of oil (only) lubricant (figure 8(a)). A few deeper grooves were also observed on the wear surfaces (figure 8(a), region marked by A). Sticking of fine debris and formation of pits on the wear surfaces were additional features noted (figure 8(b), regions marked by single and double arrows, respectively). The wear grooves were not well defined in the case of the cast iron

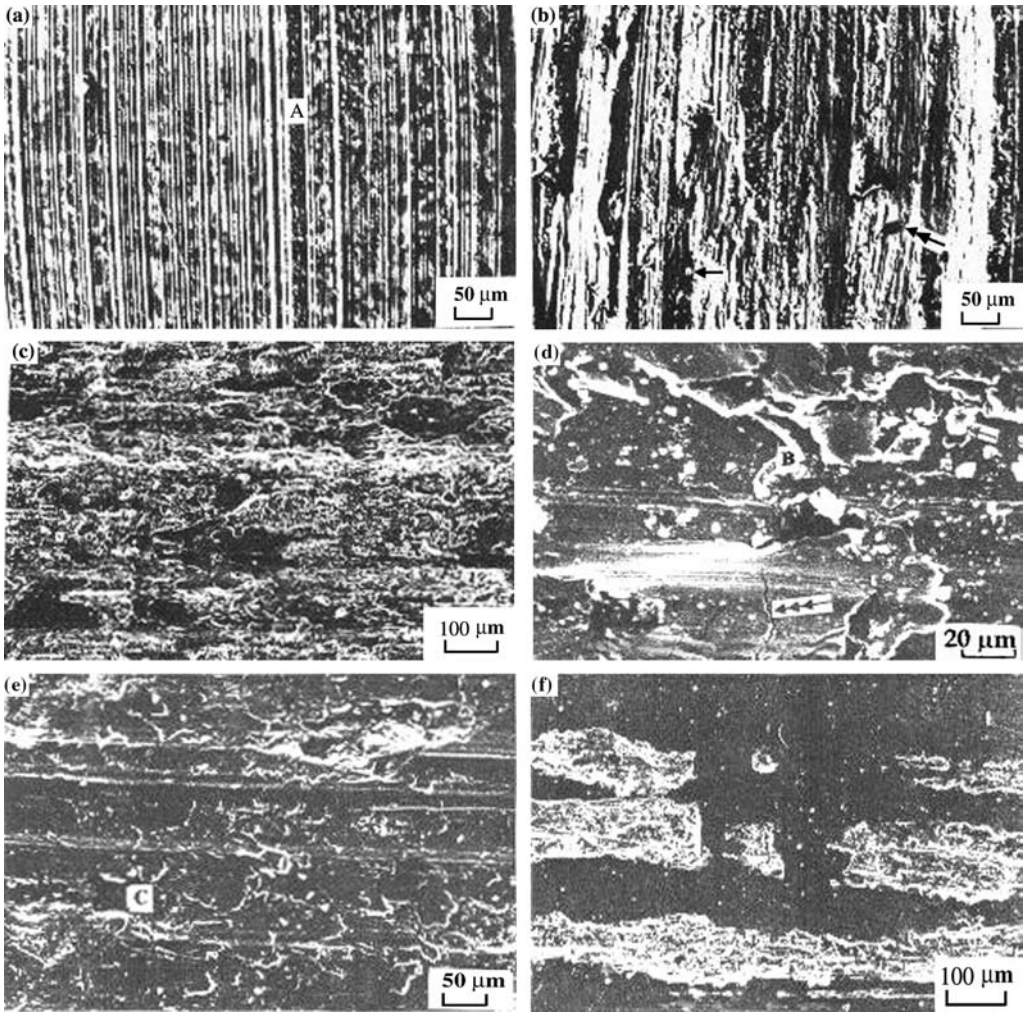

Figure 8. Wear surfaces of (a and b) the zinc-based (matrix) alloy and (c–f) cast iron tested in (a, c–e) oil and (b and f) oil plus graphite mixture [A: deeper groove, single arrow: sticking of debris, double arrow: pit, B: chip, triple arrow: microcracks, C: graphite particle exposed onto the sliding surface].

in general (figure 8(c–f)). Dark patches of smooth regions were also observed in this case (figure 8(c) and (f)). Further, the fraction of the wear surface covered by the dark regions increased substantially when tested in oil plus graphite environment (figure 8(f)) as compared to that in the case of the oil lubricant (figure 8(c)). Sticking of debris particles, entrapment of chips and microcracking on the wear surfaces of the cast iron were also noted (figure 8(d), regions marked by a single arrow, B and a triple arrow, respectively). Graphite particles present within the cast iron also got an opportunity to be exposed on the wear surface (figure 8(e), region marked by C) suggesting the smearing of the graphite particles and form a lubricating tribochemical layer [20–22] on the wear surfaces (dark patches/regions in figure 8(c) and (f)). The formation of smoother wear surfaces and more of dark patches thereon indicates better wear response of the samples (figures 3–7) and *vice versa*.

3.5. Subsurface regions

Figure 9 shows subsurface regions of the samples. The severity and degree of plastic deformation, straining and temperature cycling [52,53,65,66] experienced by the samples during sliding decreased with increasing depth below the wear surface. Accordingly, the topmost region (nearest to the wear surface) was subjected to the most severe plastic deformation causing its appearance to be white [71], as shown in figure 9(b) (region marked by a single arrow). Extremely fine microconstituents were generated in the region next to the topmost one (figure 9(a) and (e), regions marked by A). Extremely fine size of the microconstituents is clearly evident in a magnified view (figure 9(f)) of figure 9(e). Flow of microconstituents in the region undergoing less severity of deformation (than the regions marked by A in figure 9(a) and (e)) was noticed (figure 9(b),(d) and (e), regions marked by B). Deformation and stringer formation of graphite particles in the case

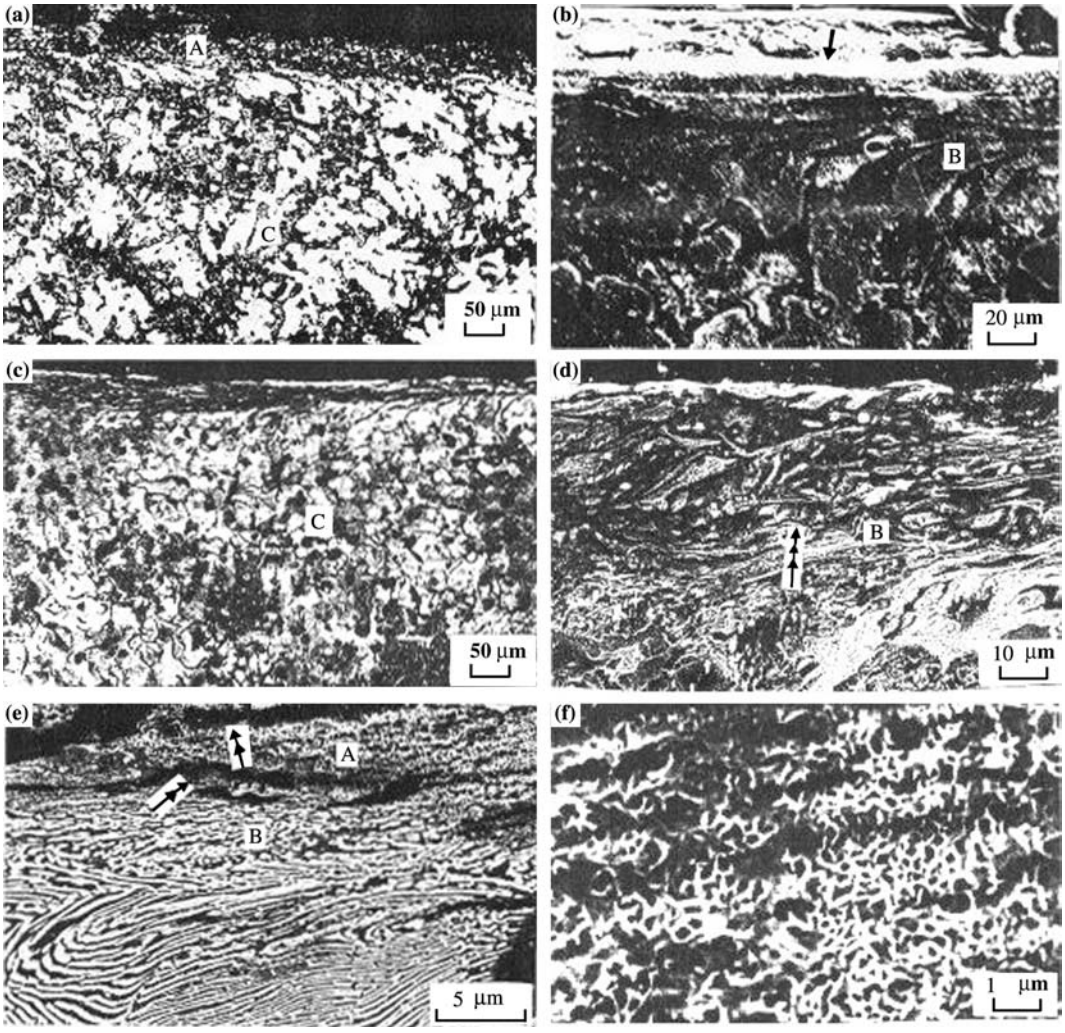

Figure 9. Subsurface regions of (a and b) the zinc-based (matrix) alloy and (c–f) cast iron tested in (a,c and d) oil and (b,e and f) oil plus graphite lubricant mixture [single arrow: white region, A: extremely fine microconstituents, B: flow of microconstituents in sliding direction, double arrow: orientation and deformation of graphite particles in sliding direction, triple arrow: microcracks, C: bulk structure].

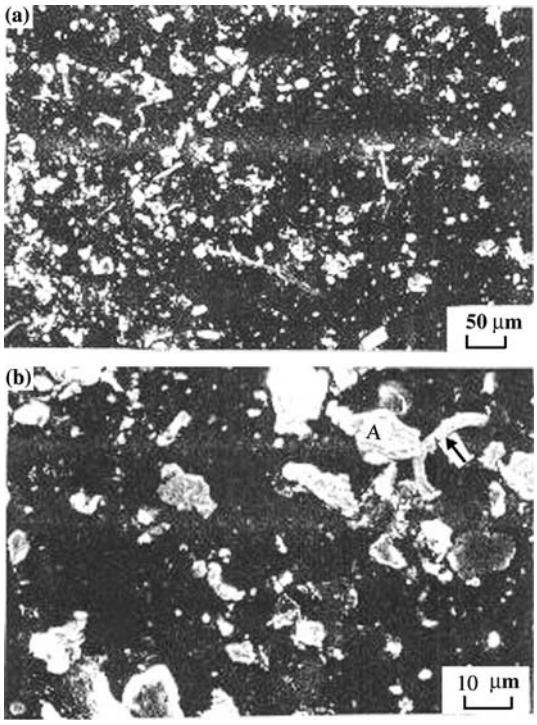

Figure 10. Wear debris showing deformed flakes and machining chips [A: flake, arrow: chip].

of the cast iron (figure 9(e), regions marked by a double arrow) indicates their tendency to smear on the wear surfaces and lubricating film formation [20–22] leading to improved wear response (figure 3–7). The presence of microcracks may be seen in figure 9(d) (region marked by a triple arrow). The region below 'B' showed normal bulk structure (figure 9(a) and (c), regions marked by C), thereby suggesting it to remain unaffected during wear.

3.6. *Wear debris*

Wear debris particles of the samples comprised deformed flakes along with a few chips (figure 10(a)). A magnified view clearly shows the flakes and chips (figure 10(b), regions marked by A and an arrow, respectively). Flaky debris particles result from the plastic deformation occurring during wear (figure 9, regions marked by arrows, A and B) while chips result from the cutting action of hard microconstituents [53].

4. Conclusions

1. The zinc-based (matrix) alloy comprised primary α dendrites and eutectoid $\alpha + \eta$ and ε in the interdendritic regions. Reinforcement of silicon carbide particles formed a mechanical mixture with the matrix without practically affecting the (matrix) microstructural features. The reinforcement phase was distributed fairly uniformly in the matrix and the dispersoid/matrix interface was reasonably sound. The cast iron revealed various sizes and modes of distribution (such as randomly dispersed, coarse and distorted flakes and interdendritic segregation and rosettes of fine flakes) of graphite in the matrix of pearlite and (a limited quantity of) ferrite.
2. The hardness and density of the cast iron were highest amongst the three varieties of the samples. The density of the composite was the least while the zinc-based (matrix) alloy exhibited minimum hardness.
3. The zinc-based (matrix) alloy exhibited highest wear rate followed by that of the cast iron and composite. In other words, incorporation of silicon carbide particles significantly improved the wear resistance of the matrix alloy, making it even superior to that of the cast iron. Inferior wear resistance (inverse of wear rate) of the cast iron, having highest overall hardness, than that of the (softer) composite, indicates that the wear performance of the samples could more effectively be explained in terms of factors like load carrying, lubricating and microcracking characteristics of various microconstituents in the specimen material rather than the overall hardness of the samples.
4. The frictional heating increased at high rates in the beginning of the tests followed by a lower rate of heating at longer test durations. The composite exhibited the highest frictional heating. Moreover, the cast iron and zinc-based (matrix) alloy attained comparable frictional heating.
5. Test duration had a mixed influence on friction coefficient. The zinc-based (matrix) alloy exhibited a lower friction coefficient than that of the cast iron at lower graphite contents in the oil. On the other hand, the trend reversed at higher graphite contents. The composite attained the highest friction coefficient over the entire range of concentrations of graphite particles in the oil lubricant.
6. The presence of graphite particles suspended in the oil lubricant significantly improved the wear response of the samples in terms of decreased wear rate, less frictional heating and reduced friction coefficient up to a critical concentration (4–6%) of graphite. The trend reversed at still higher graphite contents in the lubricant mixture. Accordingly, it emerges from the present study that the addition of graphite particles to oil lubricants becomes beneficial. However, the quantity of the suspended graphite particles in the lubricant mixture plays an important role. There exists an optimum quantity of graphite that offers the best wear performance; concentrations higher than the optimum could prove detrimental as far as the wear performance of the samples is concerned.

References

[1] T.S. Calayag, Mining Eng. 35 (1983) 727.
[2] K.J. Altorfer, Met. Prog. 34 (1982) 29.
[3] E.J. Kubel Jr., Adv. Mater. Process. 132 (1987) 51.
[4] A.A. Das, A.J. Clegg, B. Zentout and M.M. Yarkoub, in: *Proceedings of the Cast Reinforced Metal Matrix Composites*, eds. S.G. Fishman and A.K. Dhingra. (ASM International, 1988) 139.
[5] M.A. Dellis, J.P. Keustermans and F. Delannay, Mater. Sci. Eng. A, 135A (1991) 253.
[6] B.K. Prasad, S. Das, O.P. Modi, A.K. Jha, R. Dasgupta and A.H. Yegneswaran, J. Mater. Eng. Pref. 8 (1999) 693.
[7] S. Muthukumaraswamy and S.S. Seshan, Composites 26 (1995) 387.
[8] L.D. Bailey, S. Dionne and S.H.J. Lo, in: Fundamental Relationship between Microstructure and Properties of the Metal Matrix Composites, eds. P.K. Liaw and M.N. Gungor (The Minerals, Metals and Materials Society, Warrendale, PA, 1990) 23.
[9] H.X. Zhu and S.K. Liu, Composites 5 (1993) 437.
[10] N. Dahotre, T.D. McCay and M.H. McCay, J. Met. 42 (1990) 44.
[11] B.K. Prasad, A.K. Jha, S. Das, O.P. Modi, R. Dasgupta and A.H. Yegneswaran, J. Mater. Sci. Lett. 18 (1999) 1731.
[12] B.K. Prasad, Wear 254 (2003) 35.
[13] T.S. Eyre, *Metals Handbook*, Vol. 18, 10th ed., (ASM, Materials Park, Ohio, USA, 1992) 695.
[14] C.V. White, *Metals Handbook*, Vol. 1, 10th ed., (ASM, Materials Park, Ohio, USA, 1990) 12.
[15] Y. Zhang, Y. Chen, R. He and B. Shen, Wear 166 (1993) 179.
[16] M.H. Cho, S.J. Kim, R.H. Basch, J.M. Fash and H. Jang, Tribol. Int. 36 (2003) 537.
[17] A. Rac, Tribol. Int. 18 (1985) 29.
[18] H.T. Angus and A.D. Lamb, *I. Mech. Eng. Conf. on Lubrication and Wear* London, 1957.
[19] E. Takeuchi, Wear 19 (1972) 267.
[20] S. Das, S.V. Prasad and T.R. Ramachandran, Wear, 133 (1989) 173.
[21] S. Das, S.V. Prasad and T.R. Ramachandran, Mater. Sci. Eng. A 138A (1991) 123.
[22] B.K. Prasad and S. Das, Mater. Sci. Eng. A 144A (1991) 229.
[23] P.K. Rohatgi, R. Asthana and S. Das, Int. Met. Rev. 31 (1986) 115.
[24] T.S. Eyre, R.F. Iles and D.W. Gasson, Wear 13 (1969) 229.
[25] A.K. Jha, S.V. Prasad and G.S. Upadhyaya, *Proc. Wear Resistance of Metals and Alloys, Chicago, Illinois, USA, 24–30 Sept, 1988*, ed. Kingsbury, G.R. ASM, Ohio, USA, 73.
[26] S.V. Prasad and P.K. Rohatgi, J. Met. 39 (1987) 22.
[27] R.S. Montgomery, Wear 13 (1969) 337.
[28] T.S. Eyre and F. Wilson, Lubr. Eng. 29 (1973) 65.
[29] A.K. Jha, S.V. Prasad and G.S. Upadhyaya, Wear 133 (1989) 163.
[30] P.K. Rohatgi, Y. Liu and T.L. Barr, Metall. Trans. A 22A (1991) 1435.
[31] Y. Liu, P.K. Rohatgi and S. Ray, Metall. Trans. A 24A (1993) 151.
[32] Y. Nakamura and S. Hirayama, Wear 132 (1989) 337.
[33] T.H.C. Child and F. Sabbagh, Wear 134 (1989) 81.
[34] H.H. Masjuki and M.A. Maleque, Wear 198 (1996) 293.
[35] E. Takeuchi, Wear 15 (1970) 201.
[36] T.S. Eyre and C. Fitter, Wear 90 (1983) 31.
[37] G. Rowe, Wear 3 (1960) 274.
[38] J. Lancaster, Wear 34 (1975) 275.
[39] M. Brendle, J. Falkin, P. Turgis and R. Gilmore, STLE Tribo. Trans. 33 (1990) 471.
[40] J. Lancaster, Wear 9 (1966) 169.
[41] C. Langlade, S. Faveulic and R. Olifer, Appl. Surf. Sci. 65–66 (1993) 83.
[42] J. Sugishita and Fujiyoshi, Wear 66 (1981) 209.
[43] Y.B. Liu, S.C. Lim, S. Ray and P.K. Rohatgi, Wear 159 (1992) 201.
[44] P.K. Rohatgi, S. Ray, Y. Liu, Int. Mater. Rev. 37 (1992) 129.
[45] S.V. Prasad and B.D. McConnell, Wear, 149 (1991) 241–253.
[46] C. Langlade, S. Fayeulle and R. Olifer, Wear 172 (1994) 85.
[47] B.K. Prasad, A.K. Patwardhan and A.H. Yegneswaran, J. Mater. Eng. Perf. 7 (1998) 130.
[48] S.H.J. Lo, S. Dionne, M. Sahoo and H.M. Hawthorne, J. Mater. Sci. 27 (1992) 5681.
[49] G.R. Godlak and J. Gordan, J. Inst. Met. 92 (1963–1964) 230.
[50] E. Gervais, H. Levert and M. Bess, Trans. AFS 68 (1980) 183.
[51] K. Lohberg, Z. Metallkd. 74 (1983) 456.
[52] B.S. Mazumdar, A.H. Yegneswaran and P.K. Rohatgi, Mater. Sci. Eng. 68 (1984) 85.
[53] B.K. Prasad, A.K. Patwardhan and A.H. Yegneswaran, Metall. Mater. Trans. A 27A (1996) 3513.
[54] S. Murphy and T. Savaskan, Wear 98 (1984) 151.
[55] S.W.K. Morgan ed., *Zinc and Its Alloy and Compounds*, 1st ed., (Ellis Horwood, John Willey & Sons, New York, 1985) 154.
[56] E.R. Braithwaite and G.W. Rowe, Sci. Lubr. 1963, 92.
[57] T. Tsuya and R. Takagi, Wear 7 (1964) 131.
[58] R.J. Barnhurst and J.C. Farge, in: eds. G.P. Lewis, R.J. Barnhurst and C.A. Loong, *Metallurgical Society of Canadian Institute of Metals*, (Toronto, Ontario, Canada, Aug. 17–20, 1986) 85.
[59] T.J. Risdon, W.M. Mihaichuk and R.J. Barnhurst, in: *Proc. Int. Congr. Expo., SAE*, 24–28 Feb, 1986, Detroit, Michigan, Paper No. 860064.
[60] D. M. Stefanescu *Metal Handbook*, Vol. 1, 10th ed., (ASM, Materials Park, Ohio, USA, 1990) 1.
[61] H. T. Angus, ed. Cast Iron: Physical and Engineering Properties, 2nd ed. (Butterworths London, 1976) 1.
[62] A.G. Gulyaev, ed., *Physical Metallugy*, Vol. 1 (Mir Publishers, Moscow, 1980) 175.
[63] A.K. Jha, B.K. Prasad, O.P. Modi, S. Das and A.H. Yegneswaran, Wear 254 (2003) 120.
[64] J.G. Humphries, BCIRAJ 9 (1961) 609.
[65] F.E. Kennedy Jr., Wear 100 (1984) 453.
[66] D.A. Rigney, L.H. Chen, M.G.S. Naylor and A.R. Rosenfield, Wear 100 (1984) 195.
[67] P.P. Lee, T. Savaskan and E. Laufer, Wear 117 (1987) 79.
[68] M.V. Rayiko and N.F. Dmytrychenko, Wear 126 (1988) 69.
[69] J.P. Pandey and B.K. Prasad, Mater. Trans. JIM 38 (1998) 1121.
[70] O.P. Modi, B.K. Prasad, A.K. Jha, V.P. Deshmukh and A.K. Shah, Tribo. Lett. 17 (2004) 129.
[71] B.K. Prasad, Wear 151 (1991) 1.